Inorganic Chemistry

ARTICLE

pubs.acs.org/IC

Novel Lanthanide-Based Polymeric Chains and Corresponding Ultrafast Dynamics in Solution

Dominique T. Thielemann,[†] Melanie Klinger,[‡] Thomas J. A. Wolf,[‡] Yanhua Lan,[†] Wolfgang Wernsdorfer,[§] Madleen Busse,[⊥] Peter W. Roesky,*[,†] Andreas-N. Unterreiner,[‡] Annie K. Powell,[†] Peter C. Junk,[⊥] and Glen B. Deacon[⊥]

[†]Institut für Anorganische Chemie, Karlsruher Institut für Technologie (KIT), Engesserstr. 15, 76131 Karlsruhe, Germany

[‡]Institut für Physikalische Chemie, Karlsruher Institut für Technologie (KIT), Fritz-Haber-Weg 2, 76131 Karlsruhe, Germany

[§]Institut Néel, CNRS et Université Joseph Fourier, BP 166, F-38042 Grenoble Cedex 9, France

[⊥]School of Chemistry, Monash University, Melbourne, Victoria, 3800, Australia

Supporting Information

ABSTRACT: Two types of structurally related one-dimensional coordination polymers were prepared by reacting lanthanide trichloride hydrates $[LnCl_3 \cdot (H_2O)_m]$ with dibenzoylmethane (Ph_2acacH) and a base. Using cesium carbonate (Cs_2CO_3) and praseodymium, neodymium, samarium, or dysprosium salts yielded $[Cs\{Ln(Ph_2acac)_4\}]_n$ (Ln = Pr (**1**), Nd (**2**), Sm (**3**), Dy (**4**)) in considerable yields. Reaction of potassium *tert*-butoxide (KO*t*Bu) and the neodymium salt $[NdCl_3 \cdot (H_2O)_6]$ with Ph_2acacH resulted in $[K\{Nd(Ph_2acac)_4\}]_n$ (**5**). All polymers exhibit a heterobimetallic backbone composed of alternating lanthanide and alkali metal atoms which are bridged by the Ph_2acac ligands in a linear fashion. ESI-MS investigations on DMF solutions of **1**−**5** revealed a dissociation of all the five compounds upon dissolution, irrespective of the individual lanthanide and alkali metal present. Temporal profiles of changes in optical density were acquired performing pump/probe experiments with DMF solutions of **1**−**5** via femtosecond laser spectroscopy, highlighting a lanthanide-specific relaxation dynamic. The corresponding relaxation times ranging from seven picoseconds to a few hundred picoseconds are strongly dependent on the central lanthanide atom, indicating an intramolecular energy transfer from ligands to lanthanides. This interpretation also demands efficient intersystem crossing within one to two picoseconds from the S_1 to T_1 level of the ligands. Magnetic studies show that $[Cs\{Dy(Ph_2acac)_4\}]_n$ (**4**) has slow relaxation of the magnetization arising from the single Dy^{3+} ions and can be described as a single-ion single molecule magnet (SMM). Below 0.5 K, hysteresis loops of the magnetization are observed, which show weak single chain magnet (SCM) behavior.

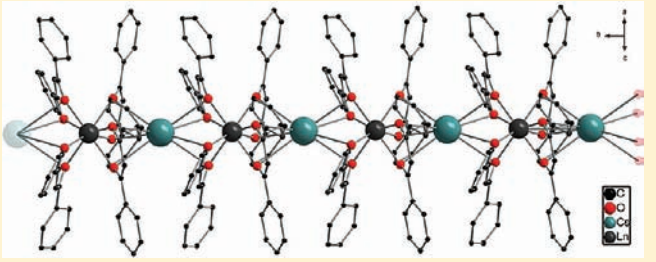

INTRODUCTION

Many applications of the lanthanides are triggered by their fascinating physical properties, which are in particular the magnetic and electronic properties of the Ln^{3+} ions.[1] In addition to the numerous applications of the solid state alloys and compounds of the lanthanides (e.g., strong permanent magnets,[2] phosphors in color TV[3]), some coordination compounds are used commercially today (e.g., MRI contrast reagents,[4−7] NMR shift reagents[8]). The unique physical properties of the lanthanides are a result of the characteristic luminescence and large anisotropic magnetic moments observed for most of these metal ions. The magnetic properties originate from the large number of unpaired 4*f* electrons and their strong spin−orbit coupling. In supramolecular chemistry many coordination polymers of the lanthanides with unique structural motifs, which are a result of high and variable coordination numbers, have been synthesized.[9] These compounds not only possess interesting structural motifs but also significant optical and magnetic properties.[10−12] One class of compounds that has recently fascinated some research groups are the so-called single chain magnets (SCM),[13,14] which are one-dimensional molecular polymeric materials that display slow relaxation of the magnetization. At low temperatures, they provide a magnetic hysteresis behavior within a single polymeric chain. The first lanthanide based SCM is the acetylacetonate ligated compound $[Dy(hfa)_3\{NIT(C_6H_4OPh)\}]$ (hfa = hexafluoroacetylacetonate; NIT(R) = 2-(4′-*R*)-4,4,5,5-tetramethylimidazoline-1-oxyl-3-oxide).[15] This compound shows slow magnetic relaxation and a dynamical crossover resulting from finite-size effects and a very pronounced static magnetic behavior. Acetylacetonate based *d*-*f* coordination polymers also show interesting luminescent properties,[16] e.g. Pt-Ln coordination polymers can be used to sensitize near-infrared luminescence at the lanthanide centers.[17] Although a huge number of investigations on

Received: May 30, 2011
Published: November 08, 2011

luminescent properties of the lanthanides has been performed,[18,19] only a few reports featuring time-resolved spectroscopic properties of lanthanide-based coordination compounds on the femtosecond scale have hitherto been published. The first time-resolved investigations with 20 ps time resolution on lanthanide porphyrin systems can be traced back to the 1980s.[20] Very recent studies on trivalent Er- and Gd-quinolinolate complexes with a much better time resolution revealed ultrafast intersystem crossing (ISC) within ten ps and a subsequent energy transfer from ligand to metal within 100 ps.[21]

The first lanthanide acetylacetonate-based complex that was identified by single crystal X-ray techniques back in 1957 was the cerium(IV) dibenzoylmethanide (Ph_2acac) compound [Ce-($Ph_2acac)_4$)].[22] To the best of our knowledge, the first structurally characterized polymeric chains of yttrium and the lanthanides with acetylacetonate-based ligands were reported in the late sixties. Two groups succeeded in isolating the heterobimetallic one-dimensional coordination polymers $[Cs\{M(hfa)_4\}]$ (M = Y,[23] Eu[24] and Am[24]) with a backbone composed of alternating yttrium, europium or americium and cesium atoms, which were bridged by hfa ligands. These compounds form zigzag chains in the solid state.

Recently, we started to investigate physical properties of easily accessible and air-stable lanthanide coordination compounds. As part of this concept we aim to obtain our compounds as single crystals in good yields without the need for any special techniques such as Schlenk apparatus or hydrothermal synthesis, and employing easily accessible or commercially available starting materials. In this context, we and others have established the synthesis of lanthanide hydroxy clusters in organic solvents using Ph_2acac as supporting ligand which is derived from acetylacetonate.[25−32] Since it is known that acetylacetonate-ligated lanthanide coordination compounds show intriguing optical[17,19] and magnetic properties,[17] we were interested in studying analogous Ph_2acac based systems. Herein we report on the synthesis and structural characterization of the one-dimensional coordination polymers $[Cs\{Ln(Ph_2acac)_4\}]_n$ (Ln = Pr, Nd, Sm, Dy) and $[K\{Nd(Ph_2acac)_4\}]_n$,[33] and the results of magnetic studies and femtosecond laser spectroscopic investigations.

EXPERIMENTAL SECTION

General Considerations. The lanthanide salts were synthesized from their corresponding oxides by reaction with concentrated hydrochloric acid, followed by evaporation to dryness. Dibenzoylmethane, cesium carbonate, potassium *tert*-butoxide and the solvents (methanol, p.a. grade) were used as purchased from commercial sources without further purification. Elemental analyses given in percent were carried out using an Elementar Vario EL at the Institute of Inorganic Chemistry at the Karlsruhe Institute of Technology (D) or an Elementar Vario Microcube at the Campbell Microanalytical service at the University of Otago (NZL). Infrared (IR) spectra were obtained using a Bruker IFS 113 v spectrometer via the attenuated total reflection method (ATR). Raman spectra were measured on a Jobin Yvon Labram spectrometer. The spectroscopic positions of the absorption bands (IR) and intensity sets (Raman) are both given in cm^{-1}. Electrospray ionization mass spectrometry (ESI-MS) was conducted with a Varian IonSpec Ultima FTICR (Fourier transformed ion cyclotron resonance) spectrometer equipped with a 7 T magnet. All signal sets of MS experiments are given in *m*/*z*. Magnetic susceptibility measurements of **4** were obtained with a Quantum Design SQUID magnetometer MPMS-XL. Micro-SQUID measurements were performed on a single crystal of **4** using an array of micro-SQUIDs.[34,35] ac-Susceptibility measurements were run with an oscillating ac field of 3 Oe and ac frequencies from 1 to 1500 Hz. Magnetic data were corrected for sample holder and the diamagnetic contribution.

General Procedure for the Synthesis of $[Cs\{Ln(Ph_2acac)_4\}]_n$ (Ln = Pr (1), Nd (2), Sm (3), Dy (4))[33]. To a stirred solution of cesium carbonate (Cs_2CO_3) (2.63 g, 8.00 mmol, 4 equiv) in 20 mL of methanol, dibenzoylmethane (Ph_2acacH) (1.83 g, 8.00 mmol, 4 equiv) was added. Subsequent dropwise addition of $[LnCl_3\cdot(H_2O)_m]$ (Ln = Pr, 746 mg (*m* = 7); Nd, 717 mg (*m* = 6); Sm, 730 mg (*m* = 6); Dy, 754 mg (*m* = 6), 2.00 mmol, 1 equiv) in 20 mL of methanol induced precipitation of a bluish solid. After stirring the reaction mixture overnight, the precipitate was separated *via* filtration and washed with 3 × 10 mL of methanol and then dried in vacuo. The desired polymeric *ate*-compounds were obtained *via* crystallization from either a hot concentrated THF/DMF solution (volume ratio: 1/5) (for Ln = Pr (**1**)) or from slow diffusion of diethyl ether into a concentrated DMF solution (for Ln = Nd (**2**), Sm (**3**) and Dy (**4**)) to give green (**1**) or yellow (**2**−**4**) needle-shaped crystals of $[Cs\{Ln(Ph_2acac)_4\}\cdot(C_3H_7NO)_2]_n$ **1**−**4** after two days.

1. Yield (single crystals): 1.43 g (55%). Anal. Calcd for $C_{60}H_{44}CsPrO_8\cdot(C_3H_7NO)_2$: C, 60.37; H, 4.45; N, 2.13. Found: C, 60.01; H, 4.24; N, 1.75. ESI-MS (DMF) *m*/*z*: 1033.228 (100%) $[M - Cs]^-$. IR [cm^{-1}]: 1677, 1593, 1543, 1509, 1476, 1455, 1384, 1301, 1279, 1219, 1180, 1154, 1083, 1066, 1058, 1022, 1000, 990, 939, 926, 847, 811, 782, 749, 715, 683, 617, 606. Raman [cm^{-1}]: 3064, 1597, 1566, 1514, 1491, 1444, 1318, 1284, 1222, 1184, 1157, 1062, 1026, 1003, 942, 794, 619.

2. Yield (single crystals): 700 mg (34%). Anal. Calcd for $C_{60}H_{44}CsNdO_8\cdot(C_3H_7NO)_{1.5}$: C, 60.53; H, 4.29; N, 1.64. Found: C, 60.23; H, 4.18; N, 1.65. ESI-MS (DMF) *m*/*z*: 1036.204 (100%) $[M - Cs]^-$. IR [cm^{-1}]: 1667, 1594, 1547, 1513, 1477, 1460, 1416, 1305, 1280, 1220, 1179, 1155, 1067, 1058, 1023, 1000, 940, 925, 847, 811, 782, 740, 721, 689, 618, 607. Raman [cm^{-1}]: 3065, 1597, 1569, 1514, 1492, 1445, 1378, 1318, 1282, 1223, 1184, 1159, 1062, 1003, 942, 794, 619.

3. Yield (single crystals): 1.88 g (84%). Anal. Calcd for $C_{60}H_{44}CsSmO_8\cdot(C_3H_7NO)$: C, 60.57; H 4.11; N 1.12. Found: C, 60.41; H, 3.95; N, 0.92. ESI-MS (DMF) *m*/*z*: 1046.234 (100%) $[M - Cs]^-$. IR [cm^{-1}]: 1677, 1594, 1546, 1512, 1477, 1309, 1281, 1220, 1179, 1155, 1089, 1067, 1060, 1022, 1000, 940, 928, 847, 811, 783, 748, 740, 719, 689, 660, 618, 608. Raman [cm^{-1}]: 3064, 1597, 1568, 1514, 1491, 1445, 1318, 1284, 1222, 1184, 1157, 1125, 1062, 1027, 1003, 942, 869, 794, 687, 619.

4. Yield (single crystals): 1.40 g (58%). Anal. Calcd for $C_{60}H_{44}CsDyO_8\cdot(C_3H_7NO)_{0.2}$: C, 60.50; H, 3.80; N 0.23. Found: C, 60.11; H, 3.64; N, 0.05. ESI-MS (DMF) *m*/*z*: 1056.227 (100%) $[M - Cs]^-$. IR [cm^{-1}]: 1678, 1595, 1548, 1510, 1478, 1456, 1419, 1397, 1311, 1301, 1281, 1220, 1180, 1155, 1061, 1023, 1000, 986, 976, 940, 925, 848, 811, 791, 783, 749, 739, 716, 689, 683, 617, 608. Raman [cm^{-1}]: 3065, 1596, 1514, 1492, 1445, 1318, 1283, 1222, 1184, 1160, 1063, 1028, 1002, 943, 793, 688, 620.

Synthesis of $[K\{Nd(Ph_2acac)_4\}]_n$ (5) and $[Ln_4(\mu_3\text{-}OH)_2(Ph_2acac)_{10}]$ (Ln = Pr (6), Sm (7)). To a stirred solution of KO*t*Bu (1.526 g, 13.2 mmol, 4 equiv) in 40 mL of methanol, Ph_2acacH (2.96 g, 1.65 mmol, 4 equiv) was added. Subsequent dropwise addition of $[LnCl_3\cdot(H_2O)_m]$ (Ln = Pr (*m* = 7), 1.23 g; Nd (*m* = 6), 1.18 g; Sm (*m* = 6), 1.20 g, 3.30 mmol, 1 equiv) in 20 mL of methanol induced precipitation of a green (Ln = Pr, Nd) or a yellow (Ln = Sm) solid. After stirring the reaction mixture overnight, the precipitate was separated *via* filtration, washed with 3 × 10 mL of methanol and dried in vacuo. The residue was dissolved in 10 mL of dichloromethane and filtered. Layering of the resulting filtrate with 25 mL of *n*-hexane afforded the Nd-based polymer **5** as green rectangularly shaped crystals after four days, whereas single crystal X-ray analyses of the Pr- and Sm-based compounds revealed the formation of the literature known tetranuclear clusters $[Ln_4(\mu_3\text{-}OH)_2(Ph_2acac)_{10}]$ (Ln = Pr, Sm).[25]

5. Yield (single crystals): 164 mg (4%). Anal. Calcd for $C_{60}H_{44}KNdO_8$: C, 66.95; H, 4.12. Found: C, 66.99; H, 4.14. ESI-MS (DMF) *m*/*z*: 1037.220 (100%) $[M - K]^-$. IR [cm^{-1}]: 3649, 3060, 2324, 1756, 1593,

Table 1. Crystallographic Data for 1−5[a]

	1·(C_3H_7NO)$_2$	2·(C_3H_7NO)$_2$	3·(C_3H_7NO)$_2$	4·(C_3H_7NO)$_2$	5·(CH_2Cl_2)$_2$
formula	$C_{60}H_{44}CsO_8Pr$·2(C_3H_7NO)	$C_{60}H_{44}CsNdO_8$·2(C_3H_7NO)	$C_{60}H_{44}CsO_8Sm$·2(C_3H_7NO)	$C_{60}H_{44}CsDyO_8$·2(C_3H_7NO)	$C_{60}H_{44}KNdO_8$·2(CH_2Cl_2)
formula mass	1312.96	1316.29	1322.40	1334.55	1246.14
crystal system	monoclinic	monoclinic	monoclinic	monoclinic	monoclinic
space group	*C*2/*c*	*C*2/*c*	*C*2/*c*	*C*2/*c*	*C*2/*c*
a (Å)	30.013(6)	30.002(7)	30.220(6)	30.068(6)	27.736(6)
b (Å)	7.9260(16)	7.9126(16)	8.0017(16)	7.9123(16)	7.9106(16)
c (Å)	26.201(5)	26.166(9)	26.115(5)	25.811(5)	26.035(5)
β (deg)	114.24(3)	114.08(3)	114.15(3)	113.84(3)	108.93(3)
V (Å^3)	5683(2)	5671(3)	5762(2)	5617(2)	5403.4(19)
T (K)	150(2)	150(2)	206(2)	150(2)	153(2)
Z	4	4	4	4	4
radiation type	Mo Kα	Mo Kα	Mo Kα	Mo Kα	Mo Kα
μ (mm^{-1})	1.551	1.611	1.704	2.033	1.293
reflections measured	27 789	56 917	68 177	38 923	55 177
independent reflections	7662	7643	7768	6451	6431
R_{int}	0.2083	0.1960	0.1065	0.1747	0.1296
*R*1 ($I > 2\sigma(I)$)[b]	0.1153	0.0423	0.1106	0.1064	0.0834
w$R(F^2)$ (all data)[c]	0.3242	0.0981	0.3034	0.2880	0.2200
goodness of fit	0.999	0.896	1.104	1.097	1.140

[a] All data were collected with Mo Kα radiation (λ = 0.71073 Å). [b] $R1 = \Sigma||F_o| - |F_c||/\Sigma|F_o|$. [c] $wR = \{\Sigma w(F_o^2 - F_c^2)^2/\Sigma[w(F_o)^2]\}^{1/2}$.

1539, 1510, 1476, 1453, 1377, 1309, 1221, 1058, 1022, 938, 783, 783, 743, 713, 681, 617. Raman [cm^{-1}]: 3065, 1596, 1567, 1514, 1492, 1444, 1359, 1319, 1286, 1223, 1183, 1163, 1062, 1028, 1002, 942, 619.

Synthesis of [Ln$_4$(μ_3-OH)$_2$(Ph_2acac)$_{10}$] (Ln = Pr (6), Nd (7)).[33] The cluster compounds were prepared upon application of literature procedures by reacting the salts [$PrCl_3$·(H_2O)$_7$] or [$NdCl_3$·(H_2O)$_6$] with 2.5 equiv Ph_2acacH in the presence of triethylamine in methanol.[25] After working up these reactions, determination of the unit cell constants of the obtained single crystals via single crystal X-ray diffraction confirmed the desired formation of clusters **6** and **7**.

X-ray Crystallographic Studies of 1−5. A suitable crystal of each of the compounds **1**−**5** was covered in mineral oil (Aldrich) and mounted onto a glass fiber. The crystal was transferred directly to the cold N_2 stream of a Stoe IPDS 2 or an Enraf Nonius Kappa CCD diffractometer.

All structures were solved by the Patterson method (SHELXS-97).[36] The remaining non-hydrogen atoms were located from successive difference Fourier map calculations. The refinements were carried out by using full-matrix least-squares techniques on F^2, minimizing the function $(F_o - F_c)^2$, where the weight is defined as $4F_o^2/2(F_o^2)$ and F_o and F_c are the observed and calculated structure factor amplitudes using the program SHELXL-97.[36] The hydrogen atom contributions of compounds **1**−**5** were calculated, but not refined. The locations of the largest peaks in the final difference Fourier map calculation as well as the magnitude of the residual electron densities in each case were of no chemical significance. Because of twinning problems high residual electron densities were observed close to the heavy atoms in some structures. The final values of refinement parameters are given in Table 1.

Experimental Setup for Femtosecond Laser Spectroscopy and Sample Preparation. A commercial CPA-laser-system (CPA2210, Clark-MXR) served as a source for femtosecond laser pulses. Excitation wavelengths were provided by second (388 nm) and third (258 nm) harmonic generation, respectively. Probe pulses with duration of about 60 fs in the range from 500 to 1100 nm were established by a noncollinear parametric amplifier (NOPA, Clark-MXR).

In order to conduct time-resolved pump/probe measurements, compounds **1**−**5** as well as the potassium salt of the ligand [K(Ph_2acac)] were dissolved in DMF. In solution the compounds are assumed to exist in their monomeric form. For further investigations the previously reported cluster compounds [Ln$_4$(μ_3-OH)$_2$(Ph_2acac)$_{10}$] (Ln = Pr (**6**), Nd (**7**)) were dissolved in methanol. All samples were stored in a fused silica cell with an optical length of 1 mm.

A more detailed description can be found in the Supporting Information as well as in a related article.[37]

RESULTS AND DISCUSSION

Synthesis and Characterization. Reaction of one equivalent of various lanthanide trichloride hydrates [$LnCl_3$·(H_2O)$_m$] (m = 7 for Ln = Pr; m = 6 for Ln = Nd, Sm, Dy) with four equivalents of dibenzoylmethane (Ph_2acacH) and cesium carbonate (Cs_2CO_3) each afforded the one-dimensional (1D) coordination polymers [Cs{Ln(Ph_2acac)$_4$}]$_n$ (Ln = Pr (**1**), Nd (**2**), Sm (**3**), and Dy (**4**)) (Scheme 1) as large single crystals.[33] These compounds are isostructural.

These polymeric compounds display a heterobimetallic backbone which is made up by the cesium atom and the individual lanthanide atom in an alternating fashion, held together by bridging dibenzoylmethanide (Ph_2acac) ligands. Adjacent metal atoms are each bridged by a set of two Ph_2acac ligands, whereby each couple of Ph_2acac ligands is layer-type shaped. Each monomeric unit of **1**−**4** is composed of a [Ln(Ph_2acac)$_4$]$^-$-moiety that is charge-balanced by a cesium cation. These compounds may be assigned to the class of the *ate*-complexes in which monomeric *ate*-units are linearly assembled to give infinite polymeric chains.

Coordination polymers **1**−**4** have been characterized by standard analytical and spectroscopic techniques, and the corresponding solid state structures were established by single crystal X-ray diffraction (Figure 1). The average interatomic distances between the cesium atom and the lanthanide atom in the backbone

Scheme 1. Synthesis of $[Cs\{Ln(Ph_2acac)_4\}]_n$ with Ln = Pr (1), Nd (2), Sm (3) and Dy (4)

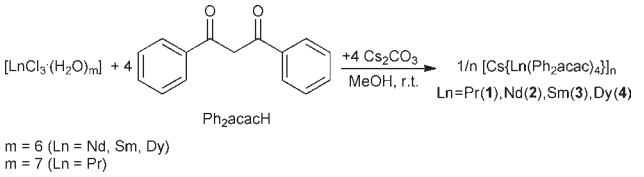

of the polymers **1**−**4** is 3.970 Å, with only marginal deviations among the compounds (3.9589(15) Å (**1**), 3.9474(10) Å (**2**), 4.0040(12) Å (**3**) and 3.9518(12) Å (**4**)). The Ln−Cs−Ln angle of 180.0° in all four compounds **1**−**4** is evident for the linear shape of the backbones.

The lanthanide atoms in **1**−**4** are chelated by all four Ph_2acac ligands, hence, they exhibit a coordination number of eight (Figure 1). The donating oxygen atoms around the lanthanide atoms display a regular square antiprismatic arrangement providing D_{4d} point symmetry, which arises from the staggered conformation of adjacent Ph_2acac layers positioned between both types of metal atoms. The Ph_2acac ligands adopt the doubly bridging and chelating μ:κ^2:κ^2-coordination mode, that is, the lanthanide atom and the cesium atom are bridged and chelated by both Ph_2acac oxygen atoms each. As a result, the symmetric arrangement of the Ph_2acac ligands around the lanthanide atoms is reflected in very similar lanthanide-oxygen bond distances, that is, they deviate by only 0.01−0.03 Å (range of Ln−O 2.428(8)−2.457(8) Å (**1**), 2.414(3)−2.445(3) Å (**2**), 2.387(6)−2.416(6) Å (**3**), and 2.340(6)−2.351(6) Å (**4**)). The cesium atom is also chelated by each Ph_2acac ligand giving a coordination number of eight, hence, the oxygen atoms also display a square antiprismatic coordination polyhedron around the cesium atom. This aspect is mirrored by very similar bond distances between the cesium atom and the oxygen atoms (range of Cs−O 3.265(9)−3.302(8) Å (**1**), 3.250(3)−3.301(3) Å (**2**), 3.281(7)−3.359(7) Å (**3**), and 3.261(7)−3.338(7) Å (**4**)).

The $[Cs\{Ln(Ph_2acac)_4\}]$ moieties described assemble linearly and are infinitely repeated along the *b*-axis to give the chainlike 1D-coordination polymers **1**−**4** (Figure 2). In all four cases, there are no hydroxy and/or oxo ligands present in the coordination sphere of the lanthanide atoms. This appears surprising since we and numerous groups have shown that experiments applying similar reaction conditions with differing stoichiometries give multinuclear cluster compounds possessing a certain content of hydroxy or oxo ligands.[25−28,30,31,38−42]

In contrast to compounds **1**−**4**, the heterobimetallic 1D-coordination polymers $[Cs\{M(hfa)_4\}]$ (M = Y,[23] Eu,[24] Am;[24] hfa = hexafluoroacetylacetonate) are not aligned in a linear but in a zigzag fashion, which is reflected by bond angles between the backbone members of Cs−Eu−Cs 153.466(8)°[24] and Cs−Y−Cs 154.399(10)°,[23] respectively (in **1**−**4**: 180.0°). Another contrast to the herein reported polymers **1**−**4** is indicated by the coordination environment of the cesium atom in $[Cs\{Y(hfa)_4\}]$, which is exclusively made up by ligand-derived fluorine atoms, and the four hfa ligands solely chelate the yttrium atom with their oxygen atoms in κ^2-mode.[23] In $[Cs\{Eu(hfa)_4\}]$ and $[Cs\{Am(hfa)_4\}]$, the europium and americium atoms are also chelated by each hfa ligand in κ^2-mode. Two out of the four hfa ligands bridge adjacent metal atoms in μ:κ^2:κ^2-mode,

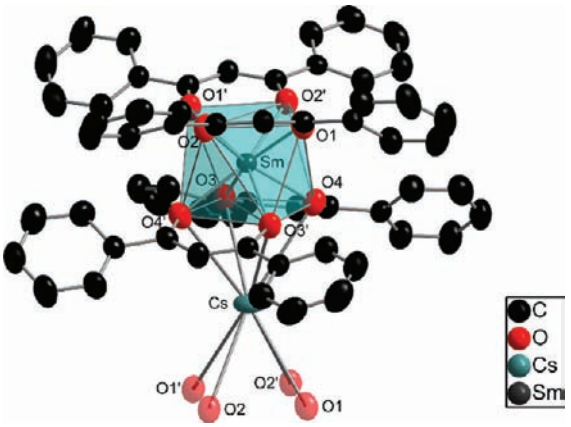

Figure 1. Thermal ellipsoid plot of one monomeric unit of the molecular structure of $[Cs\{Ln(Ph_2acac)_4\}]_n$, exemplified for **3**. Thermal ellipsoids are drawn at the 50% probability level. Hydrogen atoms are omitted for clarity. Semitransparent atoms belong to adjacent monomeric unit. Polymers **1**, **2**, and **4** are isostructural with **3**. Selected distances [Å] and angles [deg] for **1**−**4**: **1** (Ln = Pr) Pr−Cs 3.9589(15), Pr−O1 2.429(7), Pr−O2 2.439(7), Pr−O3 2.428(8), Pr−O4 2.457(8), Cs−O1 3.302(8), Cs−O2 3.267(8), Cs−O3 3.265(9), Cs−O4 3.267(9); Pr−Cs−Pr 180.0, O1−Pr−O2 69.0(2), O3−Pr−O4 68.3(2), Pr−O1−Cs 86.2(2), Pr−O2−Cs 86.8(2), O1−Cs−O2 49.7(2), O3−Cs−O4 49.2(2), Cs−O3−Pr 86.8(2), Cs−O4−Pr 86.3(2); **2** (Ln = Nd) Nd−Cs 3.9474(10), Nd−O1 2.414(3), Nd−O2 2.445(3), Nd−O3 2.431(3), Nd−O4 2.416(3), Cs−O1 3.250(3), Cs−O2 3.272(3), Cs−O3 3.258(3), Cs−O4 3.301(3); Nd−Cs−Nd 180.0, O1−Nd−O2 68.91(10), O3−Nd−O4 69.14(10), Nd−O1−Cs 87.04(9), Nd−O2−Cs 86.05(8), O1−Cs−O2 49.86(7), O3−Cs−O4 49.58(7), Cs−O3−Nd 87.09(8), Cs−O4−Nd 86.35(9); **3** (Ln = Sm) Sm−Cs 4.0040(12), Sm−O1 2.387(6), Sm−O2 2.416(6), Sm−O3 2.405(6), Sm−O4 2.396(6), Cs−O1 3.311(7), Cs−O2 3.299(7), Cs−O3 3.281(7), Cs−O4 3.359(7); Sm−Cs−Sm 180.0, O1−Sm−O2 69.5(2), O3−Sm−O4 69.7(2), Sm−O1−Cs 87.2(2), Sm−O2−Cs 87.4(2), O1−Cs−O2 48.74(15), O3−Cs−O4 48.77(15), Cs−O3−Sm1 88.2(2), Cs−O4−Sm 86.5(2); **4** (Ln = Dy) Dy−Cs 3.9518(12), Dy−O1 2.351(6), Dy−O2 2.348(6), Dy−O3 2.340(6), Dy−O4 2.344(6), Cs−O1 3.261(7), Cs−O2 3.338(7), Cs−O3 3.295(7), Cs−O4 3.277(7); Dy−Cs−Dy 180.0, O1−Dy−O2 71.1(2), O3−Dy−O4 70.6(2), Dy−O1−Cs 88.3(2), Dy−O2−Cs 86.5(2), O1−Cs−O2 48.86(15), O3−Cs−O4 48.7(2), Cs−O3−Dy 87.4(2), Cs−O4−Dy 87.8(2).

whereas the other two ligands adopt the μ:κ^2-mode.[24] As a consequence, the cesium atom is "only" coordinated by a total of six oxygen atoms (compared to eight in compounds **1**−**4**), in addition to six hfa-derived fluorine atoms.

As we succeeded in preparing novel polymeric coordination compounds **1**−**4** by using a cesium containing base and slightly modifying the reaction stoichiometry compared with that for the known tetra- and pentanuclear hydroxy clusters,[25,27−30,32,38,39,43,44] we investigated the scope of other possible alkali metal derived backbone members. Furthermore, striking differences in ionic radii when comparing cesium (1.84 Å; CN = 6)[45] with, for example, potassium (1.52 Å; CN = 6)[45] regarding the same coordination numbers ought to effect certain structural changes. In this context, it appeared desirable to determine the size-related frontiers in coordination chemistry for obtaining lanthanide-based polymeric coordination compounds, such as **1**−**4**.

For this purpose, reaction of one equivalent of various lanthanide trichloride hydrates $[LnCl_3\cdot(H_2O)_m]$ (m = 7 for Ln = Pr; m= 6 for Ln = Nd, Sm) with four equivalents of

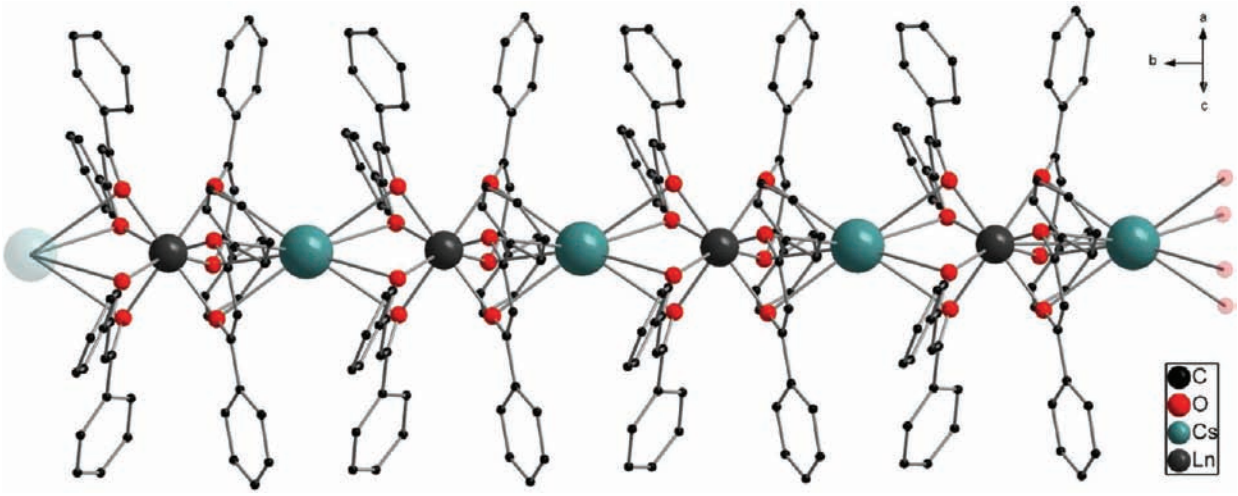

Figure 2. Assembly of several monomeric units of **1**−**4** makes up the polymeric domain along the *b*-axis. Semitransparent atoms denote peripheries of adjacent monomeric units. Hydrogen atoms are omitted for clarity.

Scheme 2. Synthesis of $[K\{Nd(Ph_2acac)_4\}]_n$ 5 and Fortuitous Syntheses of $[Ln_4(\mu_3\text{-}OH)_2(Ph_2acac)_{10}]$ with Ln = Pr, Sm[25]

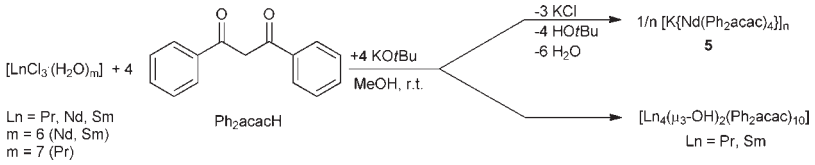

dibenzoylmethane (Ph_2acacH) was performed under the same conditions as for **1**−**4**, but using four equivalents of potassium *tert*-butoxide (KO*t*Bu) instead of Cs_2CO_3. Considering the conversion involving the neodymium salt, the solution of the corresponding solid state structure revealed the formation of a novel one-dimensional coordination polymer of formula $[K\{Nd(Ph_2acac)_4\}]_n$ (**5**) (Scheme 2). In contrast, the reaction of the praseodymium and samarium containing compounds resulted in the formation of the literature known clusters $[Ln_4(\mu_3{-}OH)_2(Ph_2acac)_{10}]$ (Ln = Pr, Sm).[25] Surprisingly, the polymeric shape was solely retained in the case of neodymium(III), which possesses an ionic radius lying between the radius of praseodymium(III) and samarium(III) when considering same coordination numbers (for CN = 6, 1.153 Å (Pr^{3+}), 1.135 Å (Nd^{3+}), 1.104 Å (Sm^{3+})).[45] The photophysical properties of these compounds is discussed later (see below).

The solid state structure of **5** was established by single crystal X-ray diffraction. It reveals that compound **5** also exhibits a heterobimetallic backbone composed of alternating neodymium and potassium atoms which are bridged by the Ph_2acac ligands. In analogy to cesium compounds **1**−**4**, the monomeric unit of **5** can be best described as an *ate*-complex, as the monoanionic $[Nd(Ph_2acac)_4]^-$-moiety is electrostatically balanced by the potassium cation. Since in the solid state the potassium cation is directly coordinated by the $[Nd(Ph_2acac)_4]^-$-moiety, **5** may also be considered as a polymeric arrangement of contact ion pairs. The coordination periphery of both metal atoms is made up by four Ph_2acac ligands.

Polymer **5** crystallizes in a monoclinic crystal system in the space group *C*2/*c*, having four molecules in the unit cell, whereby the asymmetric unit contains half a formula unit. As in compounds **1**−**4**, the Nd−K−Nd angle is 180.0°, which is indicative of its linear arrangement. The interatomic distance between the potassium and the neodymium atom of 3.955(2) Å in compound **5** is by only 0.01 Å shorter than for the cesium based polymer **2**. As this contraction lies in the error range of crystallographically obtained distance values, it appears negligible and cannot be related to the much larger ionic radius of the cesium cation compared to the potassium cation.[45] The coordination sphere of the neodymium atom is made up by four κ^2-chelating Ph_2acac ligands. In contrast to **1**−**4**, a square antiprismatic arrangement with D_{4d} point symmetry of the donating oxygen atoms around the neodymium atom is not possible, since the Ph_2acac ligands are inclined sideways. This geometric distortion is attributed to the asymmetric $\mu{:}\kappa^2{:}\kappa^1$-coordination mode of the Ph_2acac ligands, which allows only one out of the two Ph_2acac oxygen atoms to bridge the neodymium atom with the above lying potassium atom. In consequence, the coordination polyhedron displayed by the oxygen atoms surrounding the neodymium atom can rather be described as a dodecahedron (Supporting Information Figure S4). Since the potassium atom is also surrounded by four Ph_2acac ligands but only singly coordinated by each ligand, it provides a total of four bonds to Ph_2acac oxygen atoms (K−O1 2.890(5) Å and K−O4 2.914(5) Å) forming a distorted tetrahedron.

As observed for **1**−**4**, no hydroxy and/or oxo ligands are accommodated in the coordination environment of the neodymium atom. In the same fashion as in **1**−**4**, the $[K\{Nd(Ph_2acac)_4\}]$ moieties assemble linearly and are infinitely continued along the crystallographic *b*-axis to give the chainlike 1D-coordination polymer **5** (Figure 3).

Furthermore, both types of polymeric *ate*-complexes feature an incorporation of the cations of the bases into their backbone,

dx.doi.org/10.1021/ic201157m |*Inorg. Chem.* 2011, 50, 11990–12000

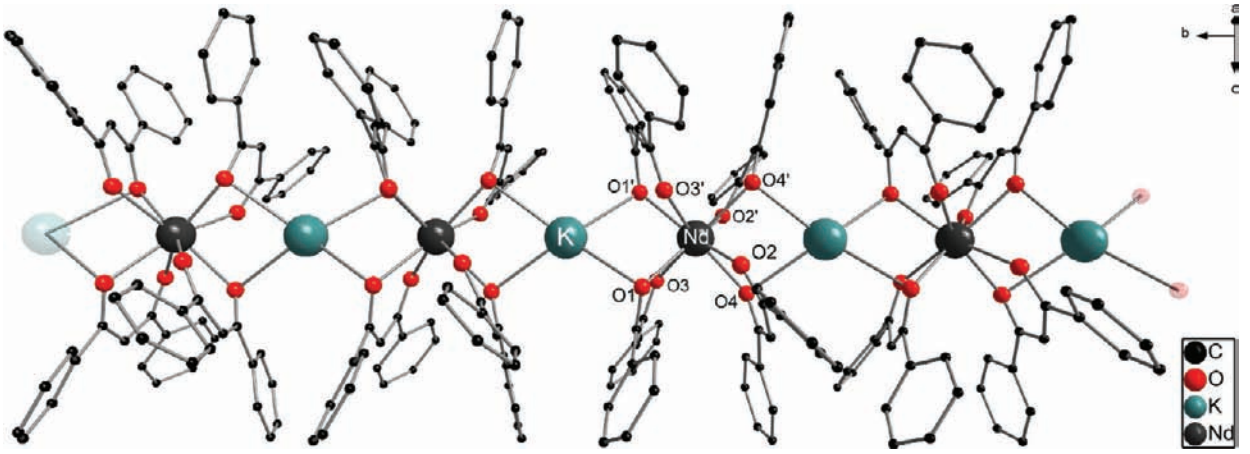

Figure 3. Assembly of several monomeric units of **5** makes up its polymeric domain along the *b*-axis of the unit cell. Semitransparent atoms denote peripheries of adjacent monomeric units. Hydrogen atoms are omitted for clarity. Selected distances [Å] and angles [deg]: Nd−K 3.955(2), Nd−O1 2.428(5), Nd−O2 2.464(5), Nd−O3 2.449(5), Nd−O4 2.409(5), K−O1 2.890(5), K−O4 2.914(5); Nd−K−Nd 180.0, O1−Nd−O2 69.6(2), O3−Nd−O4 69.1(2), Nd−O1−K 95.8(2) Nd−O4−K 95.52(15), O1−K−O1′ 75.4(2), O4−K−O4′ 74.7(2); φ = (O1−K−O1′;O4−K−O4′) = 50.068(6).

that is, the bases themselves provide an essential building block for the construction of the polymeric domains in **1**−**5**. This is obviously supported by the bridging capability and the oxophilicity of the alkali metal atoms, which allows them to act as competitive metal centers in the presence of the trivalent lanthanide ions for Ph_2acac coordination. As some groups have reported some years ago, use of various amine bases such as triethylamine,[46] 2-hydroxyethylamine,[47] *N*,*N*-dimethylbenzylamine[47] and pyrrole[47] in the presence of dibenzoylmethane and an europium(III) source exclusively yielded mononuclear charge separated ammonium *ate*-complexes of formulas $[HNEt_3][Eu(Ph_2acac)_4]$,[46] $[H_3NC_2H_4OH][Eu(Ph_2acac)_4]$,[47] $[HNMe_2Bn][Eu(Ph_2acac)_4]$,[47] and $[H_2NC_4H_4][Eu(Ph_2acac)_4]$.[47] Furthermore, some alkali metal atoms have been shown to connect transition metal based *ate*-complexes in several spatial directions for building up 2D and 3D metal organic frameworks.[48]

Subsequent electrospray ionization mass spectrometry (ESI-MS) investigations were carried out with equimolar DMF solutions of **1**−**5** (Supporting Information Figure S5−15). The resulting mass spectra for all the five compounds revealed the polymeric structure to be broken up upon dissolution in DMF, giving the monoanionic $[Ln(Ph_2acac)_4]^-$-fragments as the predominant detectable species in solution (e.g., Supporting Information Figure S5). This finding provides evidence for the instability of such lanthanide-based polymeric *ate*-complexes in solution. For all compounds, an equilibrium between the monomeric and some oligomeric species is observed, irrespective of either applying the negative (e.g., Supporting Information Figure S6) or the positive mode (e.g., Supporting Information Figure S7) on the mass spectrometer. In the case of the neodymium compounds **2** and **5**, identical signal sets derived from both the cesium (**2**) and the potassium-based polymer (**5**) in positive and negative mode indicate that their behavior in DMF solution remains unaffected by the individual alkali metal atom.

Since the tetra- and pentanuclear Ph_2acac ligated lanthanide hydroxy clusters $[Ln(\mu_3\text{-}OH)_2(Ph_2acac)_{10}]$ and $[Ln_5(\mu_4\text{-}OH)(\mu_3\text{-}OH)_4(Ph_2acac)_{10}]$ have been shown to exhibit very promising photophysical[29,43] and especially magnetic properties,[28,30] we were very interested in exploring the physical properties of compounds **1**−**5**.

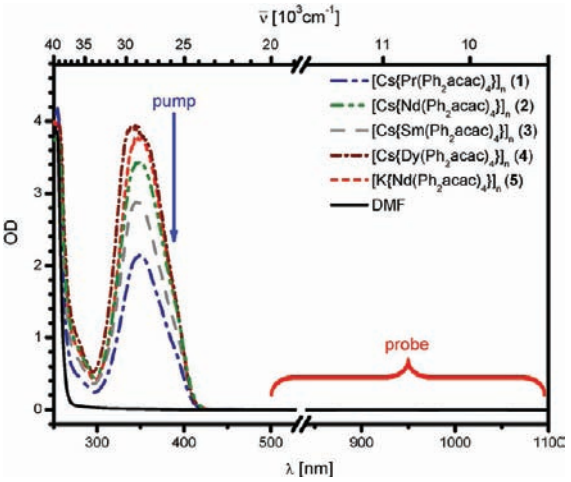

Figure 4. Steady absorption spectra of DMF solutions of **1**−**5**. The blue arrow denotes the excitation wavelength of 388 nm and the red marked region denotes the probe wavelength regime.

Femtosecond Laser Spectroscopy. Time-resolved femtosecond laser spectrospcopic experiments were performed with samples of **1**−**5** dissolved in DMF. This project was targeted on gaining first insights into ultrashort-time dynamics of such species, as certain photoinduced processes are exclusively observable on the picosecond scale. It is well-known that coordination compounds of the lanthanides in which the metal centers are coordinated by electron-rich organic ligands can show an enhanced luminescence behavior compared to free Ln^{3+} cations via the so-called "antenna effect".[18,49,50] Considerable efforts have been made to increase the luminescence quantum yields by choosing suitable ligands for the lanthanide of interest.[51−54] Therefore, ultrafast absorption spectroscopy can be crucial for a better understanding of the various pathways of energy relaxation and mechanisms of energy transfer between sensitizing ligands and central lanthanides. In principle, this method is supposed to temporally resolve each of these elementary steps by a time dependent change of the relevant absorption cross sections.

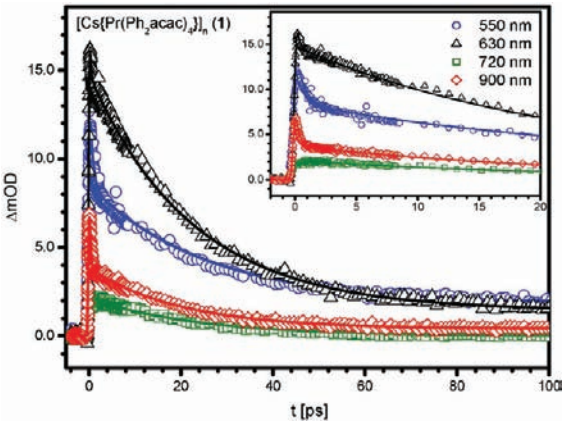

Figure 5. Time-resolved transient absorption profile of **1** in DMF after excitation with λ_{ex} = 388 nm. Probing wavelengths were λ = 550, 630, 720, and 900 nm. Symbols denote experimental values and solid lines the corresponding exponential fits.

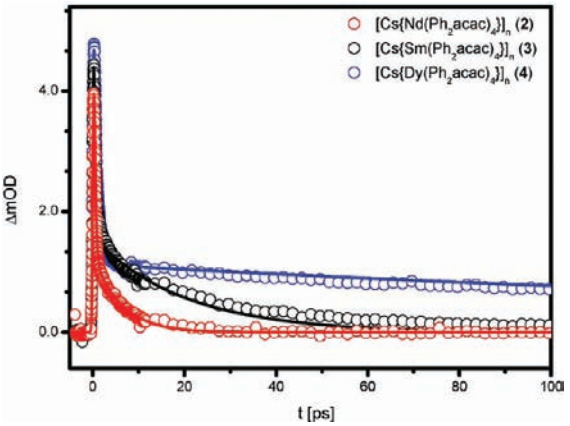

Figure 6. Time-resolved transient absorption profiles of **2**, **3**, and **4** in DMF after excitation with λ_{ex} = 388 nm and probed at 900 nm. Symbols denote experimental values and solid lines the corresponding exponential fits.

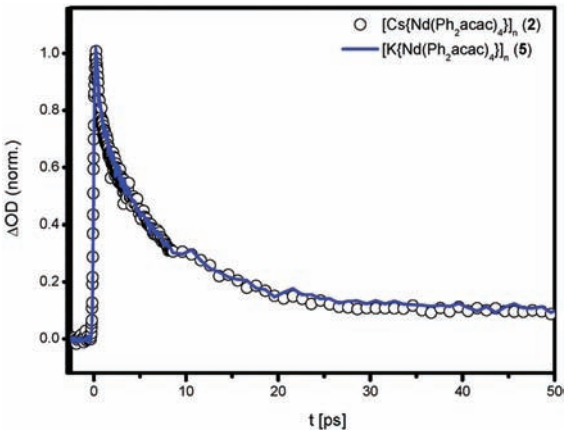

Figure 7. Time-resolved transient absorption profiles of **2** and **5** in DMF at a pump/probe wavelength combination of 388/630 nm. For easier comparison the values were normalized with respect to their maximum ΔOD value.

UV−vis absorption spectra of DMF solutions of **1**−**5** were recorded as depicted in Figure 4, where the optical density (OD) is plotted against the wavelength λ. The samples uniformly gave an absorption maximum at a wavelength of approximately 350 nm suggesting a common $\pi^* \leftarrow \pi$ transition derived from delocalized π-electrons of the Ph_2acac ligands. Beyond the almost indistinguishable absorption behavior of these compounds, photophysical degradation has been revealed to occur within approximately one week (see Supporting Information Figure S16).

On the basis of this absorption behavior, subsequent laser excitation of DMF solutions of **1**−**5** was carried out with an excitation wavelength of 388 nm. Temporal profiles resolved up to the femtosecond scale were recorded via pump/probe experiments. Figure 5 exemplifies the transient response of **1** after excitation with 388 nm in the region of the first excited singlet state (S_1) of the Ph_2acac ligands. The inset of Figure 5 represents the transients at shorter time delays in more detail. ΔOD denotes the time dependent change of the optical density of the samples. Basically a biexponential decay behavior is observable that can be related to two different time constants on the subpicosecond (τ_1) and the picosecond (τ_2) time scale, respectively. These time constants were found to be independent of the probe wavelengths. While τ_1 can tentatively be assigned to ligand relaxation processes, τ_2 obtained at different probe wavelengths (550, 630, 720, and 900 nm) is about 26 ps for **1** and can be related to lanthanide-polymer dynamics. See below for a more thorough discussion.

The transient responses of **2**-**4** (Figure 6) unambiguously show that the general relaxation behavior of these compounds after excitation of the Ph_2acac ligands exclusively depends on the individual lanthanide atom involved. Evaluation of the transients gave the following time constants for the relaxation of the lanthanide compounds: Pr, (26 ± 4) ps; Nd, (7 ± 2) ps; Sm, (21 ± 1) ps; Dy, (288 ± 50) ps (for a complete set of time constants please refer to the Supporting Information).

When comparing the relaxation behavior of the potassium and the cesium containing neodymium compounds **2** and **5**, again the same time constant of about 7 ps is observed which apparently is not influenced by the alkali metal atom (Figure 7). As previously stated by the ESI-MS findings, this aspect underlines the independence of the individual alkali metal atoms on the dissociation behavior of the polymer compounds **1**−**5**. It further shows that the spectroscopic properties of the dissolved species remain unaffected as well.

To verify the specific time constants of the polymeric lanthanide compounds, we performed a comparative experiment by using the literature known cluster compounds $[Ln_4(\mu_3\text{-}OH)_2(Ph_2acac)_{10}]$ (Ln = Pr (**6**), Nd (**7**)).[25] Therefore, initial UV−vis spectra were recorded showing the same absorption behavior as **1**, **2** and **5** (Figure 8), underlining the presence of $\pi^* \leftarrow \pi$-transitions from the Ph_2acac ligands.

Applying a pump/probe combination of 388/1065 nm **6** and **7** exhibit the same lanthanide atom specific relaxation behavior as for **1**, **2**, and **5** (Figure 9). This issue has been underlined by identical time constants (Pr = 26 ps; Nd = 7 ps) as observed for the dissolved polymer compounds **1**, **2** and **5**. In consequence, the processes which are responsible for this kind of dynamic can be assumed to be the same in the $\{Ln\}_4$-cluster compounds as in the polymeric compounds. This allows the conclusion that some kind of energy transfer between ligand and central lanthanide atom is observed.

dx.doi.org/10.1021/ic201157m |*Inorg. Chem.* 2011, 50, 11990–12000

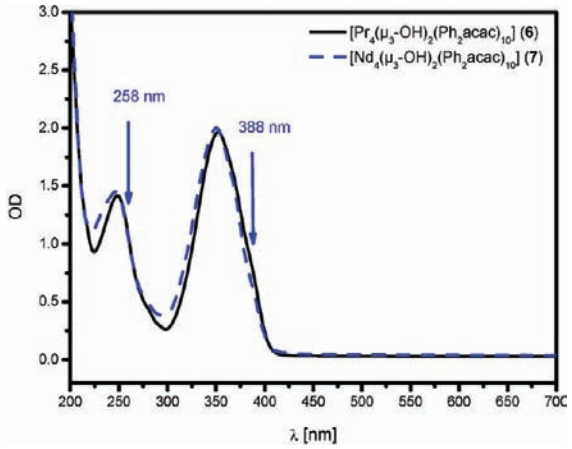

Figure 8. UV−Vis spectra of $[Ln_4(\mu_3\text{-}OH)_2(Ph_2acac)_{10}]$ (Ln = Pr (**6**), Nd (**7**)) in MeOH showing maxima at λ = 250 and 350 nm. The blue arrows denote the excitation wavelengths.

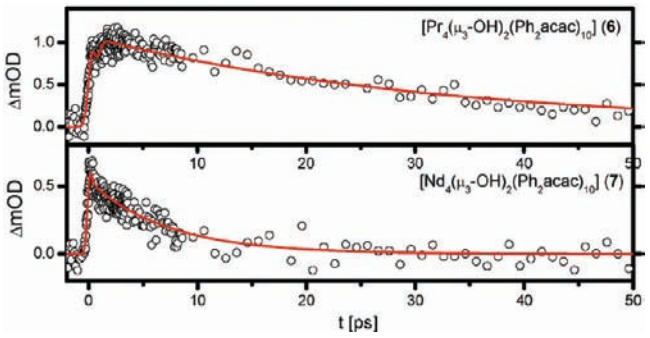

Figure 9. Temporal profiles of $[Ln_4(\mu_3\text{-}OH)_2(Ph_2acac)_{10}]$ (Ln = Pr (**6**), Nd (**7**)) in MeOH at a pump/probe combination of 388/1065 nm.

When exciting with a 258 nm pulse into the second excited singlet manifold (S_2) of the ligand, **6** and **7** show a similar temporal behavior as in the case of excitation with 388 nm, resulting in the same time constants of 26 ps for **6** and 7 ps for **7** (Supporting Information Figure S17). This observation once more suggests an energy transfer on an ultrafast time scale which is further confirmed by the different temporal behavior of the corresponding potassium salt $[K(Ph_2acac)]$ in methanol, as shown in Figure 10. For $[K(Ph_2acac)]$, only a fast monoexponential decay within 300 fs occurs upon excitation with 388 nm.

The ultrafast decay at short pump/probe delay times in the transients of **1**−**7** can now be related to a fast ligand-related relaxation dynamic followed by a much slower dynamic related to a specific energy transfer between ligand and the central lanthanide atom. At some probe wavelengths a second maximum of the ΔOD values after approximately 1 to 2 ps appears (as in Figure 9 for λ_{probe} = 1065 nm).

The mechanism of intramolecular energy transfer from electron-rich organic ligands to a central metal atom described above utilizes the "antenna effect".[55−58] A proposed interpretation of this mechanism is allowed based on time-resolved experiments: an initial ultrashort excitation of the individual solution promotes the Ph_2acac ligands from the singlet ground state (S_0) into their first excited vibrational hot singlet state S_1 (Figure 11), from which vibrational relaxation into the S_1-vibrational ground state can occur. In case of $[K(Ph_2acac)]$, the S_1 state can be depopulated

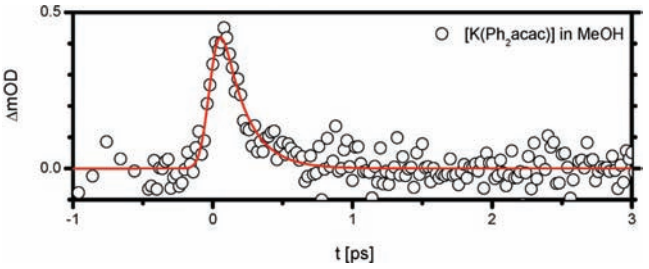

Figure 10. Temporal profile of $[K(Ph_2acac)]$ in MeOH at a pump/probe combination of 388/1065 nm.

after photoexcitation via radiationless decay or fluorescence into the S_0 ground state. Alternatively, intersystem crossing to the triplet level (T_1) can arise. The quantum yield of phosphorescence from the T_1 state apparently depends on the configuration of the ligands and whether they coordinate to metal atoms or not. In this context, it has been shown that the ligand-derived quantum yield drops down notably when going from the free ligand Ph_2acacH to the corresponding Nd^{3+} coordination complexes $[Nd(Ph_2acac)_3]$.[59] It is known that β-diketonates with an energy gap between S_1 and T_1 of about 5000 cm^{-1} exhibit efficient intersystem crossing. Based on the temporal profiles of **1**−**7**, an ultrafast intersystem crossing into the first triplet state of the ligand within one to two picoseconds (ps) can be assumed, from which the desirable ligand-to-metal charge transfer (LMCT) to an acceptor state of the lanthanide metal atom can occur.

Inspecting the time constant, τ_1, at various wavelengths and lanthanide systems (see Supporting Information, Tables S2−S7) reveals independence from the lanthanide system, but it is close to the decay of the pure ligand system, which is shown in Figure 10. Therefore, τ_1 is assigned to excited state dynamics of the ligand S_1 state (at 388 nm excitation) or S_2 state (258 nm excitation). On the other hand, the assignment of the time constant τ_2 is more complex and does depend on the coordinated polymeric lanthanide compound indicating energy transfer between ligand and the central lanthanide. Due to a variable energy gap between ligand-donor and lanthanide-acceptor states, τ_2 is determined by the individual lanthanide ion (praseodymium(III), neodymium(III), samarium(III) or dysprosium(III)). From Supporting Information Tables S2 to S7, it is clear that τ_2 is independent of the probe wavelengths throughout the visible and near-infrared spectral region and depends on the central lanthanide atom. Additionally, triplet excitation from T_1 into higher excited triplet states of the ligands may also play a role, especially in the visible region. Here, recording transient absorption spectra would be desirable, but were not possible in this work due to low overall signal intensities. Therefore, τ_2 should be interpreted as being due to a superposition of ligand-lanthanide energy transfer (LMCT) as well as the lanthanide excited state lifetime and/or triplet excitation within the ligand. For example, in the case of the praseodymium compound, τ_2 amounts to 26 ps, for the neodymium compound τ_2 is 7 ps and for the samarium coordination compound a value of 21 ps is found. The strikingly longer time constant in the case of dysprosium compound **4** (several hundreds of ps) questions the efficiency of the LMCT process to the Dy-acceptor energy levels. Furthermore, temperature dependent measurements have revealed that the energy transfer from ligand to lanthanide is more efficient at low temperatures,[60] which indicates an energy back transfer due to thermal deactivation.[61] As required by Dexter,[62] energy transfer and thermal deactivation strongly depend on the energy gap between the donor-T_1 state of

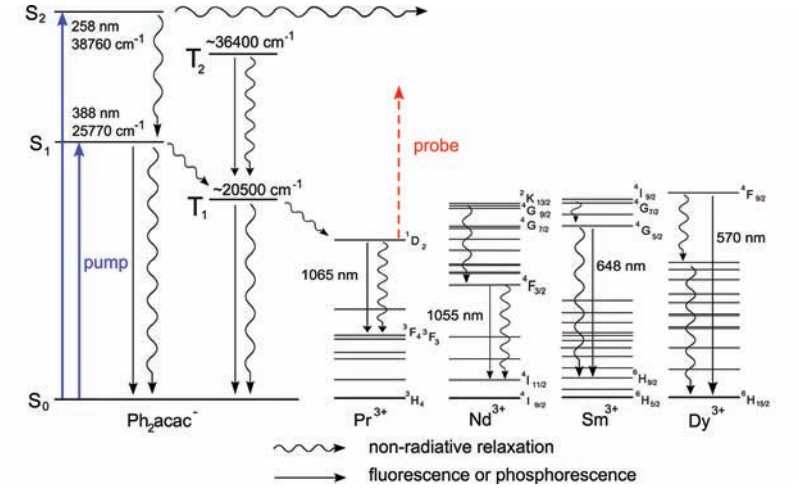

Figure 11. Extended Jablonski diagram showing possible relaxation pathways in **1**−**5**. Energy levels and emission energies from various sources.[50,54,59,69−71]

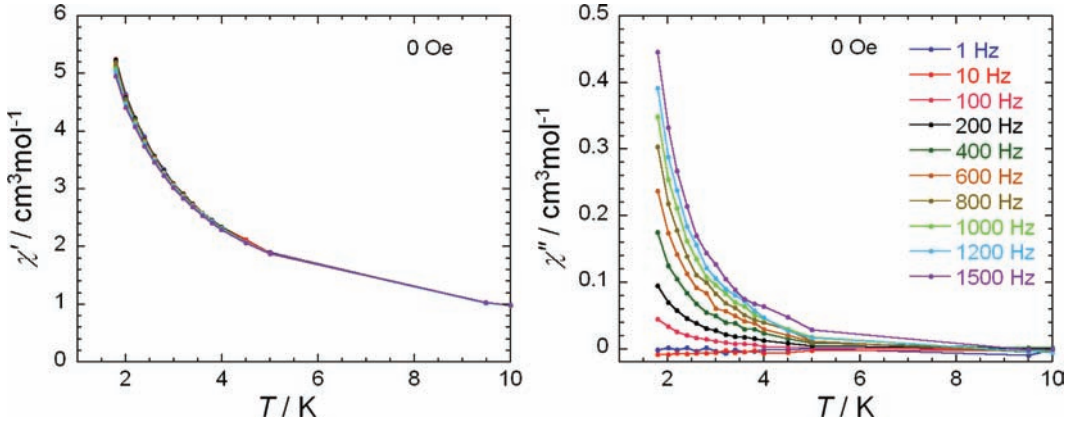

Figure 12. Temperature dependence of the in-phase (left) and out-of-phase (right) components of the ac magnetic susceptibility, for **4** under zero dc field.

the ligand and the 4*f* acceptor level of the lanthanide, which is preferably about 2500−3500 cm^{-1}.[16] For Dy-compound **4**, this energy gap seems to be small enough to efficiently promote an energy back transfer to the Ph_2acac ligands, resulting in a strikingly larger time constant when comparing with the related compounds **1**−**3** and **5**. Moreover, the spatial distance between ligand and metal atom plays an important role, not only for the LMCT process but also for the intersystem crossing transfer rate k_{ISC}, which is enhanced in the vicinity of heavy lanthanides (heavy atom effect).[63] As the differences in bond distances between the Ph_2acac derived oxygen atoms and the lanthanide atoms lie, however, in a negligible range, the elongation of the time constant of compound **4** cannot be attributed to this heavy atom effect. From these considerations, we assign the time constant τ_1 to be at least part of k_{ISC} and τ_2 to derive from the donor−acceptor transition in the lanthanide compounds **1**−**7**.

We end in pointing out that stimulated emission was also expected to be an important process besides excited state absorption (e.g., in case of Nd at 1055 nm arising from a laser-induced transition from the $^4F_{3/2}$ into the $^4I_{11/2}$ state), which would have resulted in negative ΔOD values. However, such negative values were not observed irrespective of individual conditions chosen (not even by application of a spectral confinement of the probe wavelength). On the basis of these observations, we conclude that the oscillator strength for absorption of the prepared excited states into the manifold of higher lying states is predominant. This issue might depict a general problem for accessing electronic properties in lanthanide-based coordination compounds using this method. The oscillator strength for emission could be enlarged by using ionic solvents instead of standard solvents.[64,65]

Magnetism. Magnetic studies were performed on a polycrystalline sample of **4**. As each dysprosium(III) ion is spaced by one cesium ion with a separation of 7.9 Å, the magnetic interactions between dysprosium(III) ions are likely to be very weak or negligible. The room temperature χT product of 13.82 cm^3 K mol^{-1} under an applied dc field of 0.1 T is consistent with the expected value for one isolated dysprosium(III) ion ($S = 5/2$, $L = 5$, $g = 4/3$, C = 14.17 cm^3 K mol^{-1}) (Supporting Information Figure S18). The χT product continuously decreases from room temperature until 1.8 K mainly as a result of thermal depopulation of the $^6H_{15/2}$ ground state of the dysprosium(III) ion. The field dependence of the magnetization at 2 K shows that the magnetization increases rapidly at low field and follows a linear slope above 1 T and finally reaches 5.5 μB at 7 T, indicating some anisotropy in the system (Supporting Information Figure S18, inset).

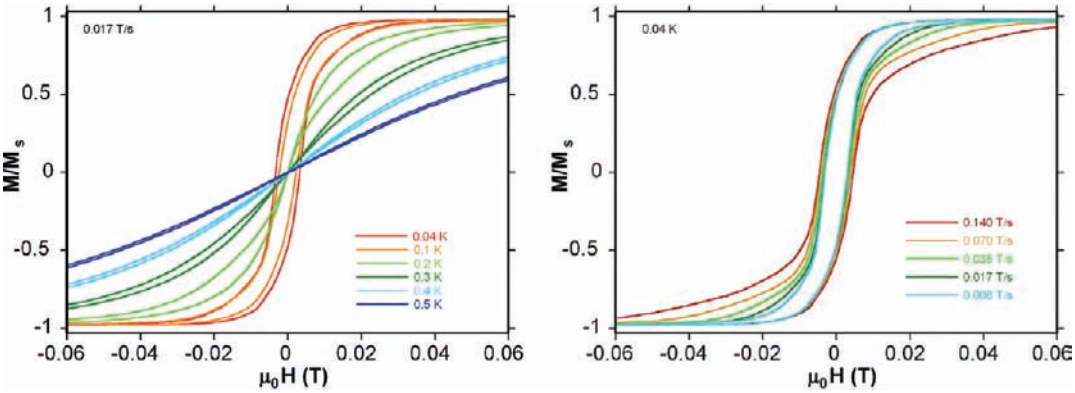

Figure 13. Normalized magnetization (M being normalized at the saturated magnetization M_S) of **4** vs applied field ($\mu_o H$). The loops are shown at different temperatures at a field sweep rate of 0.017 T/s (left) and at 0.04 K at several field sweep rates (right).

The magnetic dynamics in **4** were tested using ac susceptibility measurements under zero dc field. A nonzero frequency dependence of out-of-phase components below 6 K was detected, indicating slow relaxation of its magnetization under these conditions (Figure 12). Since no superexchange magnetic interaction is appreciable between dysprosium(III) ions, the observation of slow relaxation of the magnetization in **4** cannot be described as arising from SCM behavior but rather from the single-ion which can thus be assigned as SMM behavior originated from the Ising-type of magnetic anisotropy of single dysprosium(III) ion. In mononuclear lanthanide-based complexes exhibiting SMM behavior, the magnetic anisotropy required for observing slow relaxation of the magnetization arises from the zero-field splitting of the lanthanide ion J ground state when it is placed in a certain ligand field (LF).[66] A few mononuclear lanthanide SMMs reported so far have demonstrated that the optimum LF can be prompted if the trivalent lanthanide ion is placed in an eight-coordinate square-antiprism ligand field.[66−68] As described in the structural part, the geometry of the dysprosium atom in **4** corresponds to D_{4d} LF symmetry displaying an even square antiprismatic arrangement. Therefore, we believe that the origin of slow magnetic relaxation observed in **4** is related to the magnetic anisotropy induced by the exact symmetry of dysprosium(III) ions in such an optimum ligand field. The micro-SQUID measurements below 5 K reveal that a small hysteresis loop opens only below 0.5 K (Figure 13). The temperature and field sweep rate dependence show superparamagnetic-like behavior, that is, the hysteresis increases for decreasing temperature and increasing field sweep rate. For completely isolated dysprosium(III) ions, one would expect a strong quantum tunneling resonance at zero field. However, we observed a continuous increase for the hysteresis, typical for SCMs. Unfortunately, these interactions are too weak to be studied in detail.

SUMMARY

In conclusion, two structurally related 1D coordination polymers of formulas $[Cs\{Ln(Ph_2acac)_4\}]_n$ (Ln = Pr, Nd, Sm, Dy) and $[K\{Nd(Ph_2acac)_4\}]_n$ were obtained upon reaction of the corresponding lanthanide chloride hydrate with Ph_2acacH and either cesium carbonate or potassium *tert*-butoxide under hydrolytic conditions. Both polymer compounds highlight a heterobimetallic backbone consisting of alternating lanthanide and alkali metal cations which are fused by bridging Ph_2acac ligands. ESI-MS investigations on corresponding DMF solutions have disclosed that the dissolution of the polymers is accompanied by a uniform dissociation to their monomeric (mainly $[Ln(Ph_2acac)_4]^-$) and some oligomeric compounds, irrespective of individual lanthanide and alkali metal atoms. Pump/probe experiments of these DMF solutions applying femtosecond laser spectroscopy have revealed a lanthanide specific relaxation behavior, which is reflected in the individual temporal profiles. As shown for $[Cs\{Dy(Ph_2acac)_4\}]_n$, these investigations also demonstrate the necessity of certain energy differences between ligand-donor and lanthanide-acceptor levels, since undesirable energy back transfer (from ligand to metal) reduces luminescence quantum yields in these systems notably. Magnetic studies on dysprosium compound $[Cs\{Dy(Ph_2acac)_4\}]_n$ **4** have shown the presence of superparamagnetic-like behavior.

ASSOCIATED CONTENT

Supporting Information. Details of the ESI-MS studies, femtosecond laser spectroscopy, magnetic measurements, and X-ray crystallographic files in CIF format for the structure determinations of **1**−**5**. This material is available free of charge via the Internet at http://pubs.acs.org.

AUTHOR INFORMATION

Corresponding Author

*E-mail: roesky@kit.edu. Phone: +49/721-608-46117. Fax: 49/721-608-44854.

ACKNOWLEDGMENT

We acknowledge the financial support provided by the Deutsche Forschungsgemeinschaft (DFG) and the state of Baden-Württemberg through the DFG-Center for Functional Nanostructures within Research Area C. We are grateful to the Australian Research Council (grant DP0984775) and the Fonds der Chemischen Industrie for funding. We thank Dr. Marco Neumaier for recording ESI-MS spectra. This work is also partially supported by the ERC Advanced Grant MolNanoSpin No. 226558 and STEP MolSpinQIP.

REFERENCES

(1) Cotton, S. *Lanthanide and Actinide Chemistry*; John Wiley & Sons Ltd.: Chichester, U.K., 2006.

(2) Rodewald, W. *Rare-earth Transition-metal Magnets*; John Wiley & Sons, Ltd.: Chichester, U.K., 2007.
(3) Moine, B.; Bizarri, G. *Mater. Sci. Eng., B* **2003**, *105*, 2–7.
(4) Helm, L.; Merbach, A. E. *Chem. Rev.* **2005**, *105*, 1923–1960.
(5) Caravan, P.; Ellison, J. J.; McMurry, T. J.; Lauffer, R. B. *Chem. Rev.* **1999**, *99*, 2293–2352.
(6) Datta, A.; Raymond, K. N. *Acc. Chem. Res.* **2009**, *42*, 938–947.
(7) Bottrill, M.; Kwok, L.; Long, N. J. *Chem. Soc. Rev.* **2006**, *35*, 557–571.
(8) Lindoy, L. F. *Coord. Chem. Rev.* **1983**, *48*, 83–100.
(9) Zhou, Y.; Hong, M.; Wu, X. *Chem. Commun.* **2006**, 135–143.
(10) Cahill, C. L.; de Lill, D. T.; Frisch, M. *CrystEngComm* **2007**, *9*, 15–26.
(11) Sessoli, R.; Powell, A. K. *Coord. Chem. Rev.* **2009**, *253*, 2328–2341.
(12) Wu, M.-F.; Wang, M.-S.; Guo, S.-P.; Zheng, F.-K.; Chen, H.-F.; Jiang, X.-M.; Liu, G.-N.; Guo, G.-C.; Huang, J.-S. *Cryst. Growth Des.* **2011**, *11*, 372–381.
(13) Bogani, L.; Vindigni, A.; Sessoli, R.; Gatteschi, D. *J. Mater. Chem.* **2008**, *18*, 4750–4758.
(14) Zheng, Y.-Z.; Lan, Y.; Wernsdorfer, W.; Anson, C. E.; Powell, A. K. *Chem.—Eur. J.* **2009**, *15*, 12566–12570.
(15) Bogani, L.; Sangregorio, C.; Sessoli, R.; Gatteschi, D. *Angew. Chem., Int. Ed.* **2005**, *44*, 5817–5821.
(16) Eliseeva, S. V.; Bünzli, J.-C. G. *Chem. Soc. Rev.* **2010**, *39*, 189–227.
(17) Ronson, T. K.; Lazarides, T.; Adams, H.; Pope, S. J. A.; Sykes, D.; Faulkner, S.; Coles, S. J.; Hursthouse, M. B.; Clegg, W.; Harrington, R. W.; Ward, M. D. *Chem.—Eur. J.* **2006**, *12*, 9299–9313.
(18) Bünzli, J.-C. G. *Chem. Rev.* **2010**, *110*, 2729–2755.
(19) Moore, E. G.; Samuel, A. P. S.; Raymond, K. N. *Acc. Chem. Res.* **2009**, *42*, 542–552.
(20) Tsvirko, M. P.; Stelmakh, G. F.; Pyatosin, V. E.; Solovyov, K. N.; Kachura, T. F.; Piskarskas, A. S.; Gadonas, R. A. *Chem. Phys.* **1986**, *106*, 467–476.
(21) Quochi, F.; Saba, M.; Artizzu, F.; Mercuri, M. L.; Deplano, P.; Mura, A.; Bongiovanni, G. *J. Chem. Phys. Lett.* **2010**, *1*, 2733–2737.
(22) Wolf, L.; Bärnighausen, H. *Acta Crystallogr.* **1957**, *10*, 605–606.
(23) Bennett, M. J.; Cotton, F. A.; Legzdins, P.; Lippard, J. *Inorg. Chem.* **1968**, *7*, 1770–1776.
(24) Burns, J. H.; Danford, M. D. *Inorg. Chem.* **1969**, *8*, 1780–1784.
(25) Baskar, V.; Roesky, P. W. *Z. Anorg. Allg. Chem.* **2005**, *631*, 2782–2785.
(26) Baskar, V.; Roesky, P. W. *Dalton Trans.* **2006**, 676–679.
(27) Datta, S.; Baskar, V.; Li, H.; Roesky, P. W. *Eur. J. Inorg. Chem.* **2007**, *2007*, 4216–4220.
(28) Gamer, M. T.; Lan, Y.; Roesky, P. W.; Powell, A. K.; Clérac, R. *Inorg. Chem.* **2008**, *47*, 6581–6583.
(29) Hauser, C. P.; Thielemann, D. T.; Adlung, M.; Wickleder, C.; Roesky, P. W.; Weiss, C. K.; Landfester, K. *Macromol. Chem. Phys.* **2011**, *212*, 286–296.
(30) Andrews, P. C.; Beck, T.; Fraser, B. H.; Junk, P. C.; Massi, M.; Moubaraki, B.; Murray, K. S.; Silberstein, M. *Polyhedron* **2009**, *28*, 2123–2130.
(31) (a) Thielemann, D. T.; Fernandez, I.; Roesky, P. W. *Dalton Trans.* **2010**, *39*, 6661–6666. (b) Roesky, P. W.; Canseco-Melchor, G.; Zulys, A. *Chem. Commun.* **2004**, 738–739.
(32) Andrews, P. C.; Beck, T.; Forsyth, C. M.; Fraser, B. H.; Junk, P. C.; Massi, M.; Roesky, P. W. *Dalton Trans.* **2007**, 5651–5654.
(33) Thielemann, D. T. Dissertation Karlsruher Institut für Technologie (KIT), 2011.
(34) Cleuziou, J. P.; Wernsdorfer, W.; Bouchiat, V.; Ondarcuhu, T.; Monthioux, M. *Nat. Nano* **2006**, *1*, 53–59.
(35) Wernsdorfer, W. *Classical and Quantum Magnetization Reversal Studied in Nanometer-Sized Particles and Clusters*; John Wiley & Sons, Inc.: Chichester, U.K., 2007.
(36) Sheldrick, G. M. *Acta Crystallogr., Sect. A* **2008**, *64*, 112–122.
(37) Schalk, O.; Brands, H.; Balaban, T. S.; Unterreiner, A.-N. *J. Phys. Chem. A* **2008**, *112*, 1719–1729.
(38) Xiong, R.-G.; Zuo, J.-L.; Yu, Z.; You, X.-Z.; Chen, W. *Inorg. Chem. Commun.* **1999**, *2*, 490–494.
(39) Bürgstein, M. R.; Gamer, M. T.; Roesky, P. W. *J. Am. Chem. Soc.* **2004**, *126*, 5213–5218.
(40) Wang, R.; Zheng, Z.; Jin, T.; Staples, R. J. *Angew. Chem., Int. Ed.* **1999**, *38*, 1813–1815.
(41) Zheng, Z. *Chem. Commun.* **2001**, 2521–2529.
(42) Wang, R.; Song, D.; Wang, S. *Chem. Commun.* **2002**, 368–369.
(43) Petit, S.; Baril-Robert, F.; Pilet, G.; Reber, C.; Luneau, D. *Dalton Trans* **2009**, 6809–6815.
(44) Chen, X.-Y.; Yang, X.; Holliday, B. J. *Inorg. Chem.* **2010**, *49*, 2583–2585.
(45) Shannon, R. D.; Prewitt, C. T. *Acta Crystallogr., Sect. A* **1969**, *B25*, 925–946.
(46) Sweeting, L. M.; Rheingold, A. L. *J. Am. Chem. Soc.* **1987**, *109*, 2652–2658.
(47) Xiong, R.-G.; You, X.-Z. *Inorg. Chem. Commun.* **2002**, *5*, 677–681.
(48) Bhunia, A.; Roesky, P. W.; Lan, Y.; Kostakis, G. E.; Powell, A. K. *Inorg. Chem.* **2009**, *48*, 10483–10485.
(49) Weissman, S. I. *J. Chem. Phys.* **1942**, *10*, 214–217.
(50) Kleinerman, M. *J. Chem. Phys.* **1969**, *51*, 2370–2381.
(51) Yang, L.; Gong, Z.; Nie, D.; Lou, B.; Bian, Z.; Guan, M.; Huang, C.; Lee, H. J.; Baik, W. P. *New J. Chem.* **2006**, *30*, 791–796.
(52) Nah, M.-K.; Rho, S.-G.; Kim, H. K.; Kang, J.-G. *J. Chem. Phys. A* **2007**, *111*, 11437–11443.
(53) Meshkova, S.; Kiriyak, A.; Topilova, Z.; Antonovich, V. *J. Anal. Chem.* **2007**, *62*, 362–365.
(54) Davies, G. M.; Aarons, R. J.; Motson, G. R.; Jeffery, J. C.; Adams, H.; Faulkner, S.; Ward, M. D. *Dalton Trans.* **2004**, 1136–1144.
(55) Sato, S.; Wada, M. *Bull. Chem. Soc. Jpn.* **1970**, *43*, 1955–1962.
(56) Werts, M. H. V.; Hofstraat, J. W.; Geurts, F. A. J.; Verhoeven, J. W. *Chem. Phys. Lett.* **1997**, *276*, 196–201.
(57) Aiga, F.; Iwanaga, H.; Amano, A. *J. Phys. Chem. A* **2005**, *109*, 11312–11316.
(58) Yang, Y.; Li, J.; Liu, X.; Zhang, S.; Driesen, K.; Nockemann, P.; Binnemans, K. *ChemPhysChem* **2008**, *9*, 600–606.
(59) Song, H.; Yu, X.; Zhao, H.; Su, Q. *J. Mol. Struct.* **2002**, *643*, 21–27.
(60) Yang, C.; Fu, L.-M.; Wang, Y.; Zhang, J.-P.; Wong, W.-T.; Ai, X.-C.; Qiao, Y.-F.; Zou, B.-S.; Gui, L.-L. *Angew. Chem., Int. Ed.* **2004**, *43*, 5010–5013.
(61) Dean, C. R. S.; Shepherd, T. M. *J. Chem. Soc., Faraday Trans. 2* **1975**, *71*, 146–155.
(62) Dexter, D. L. *J. Chem. Phys.* **1953**, *21*, 836–850.
(63) Klink, S. I.; Hebbink, G. A.; Grave, L.; Oude Alink, P. G. B.; van Veggel, F. C. J. M.; Werts, M. H. V. *J. Phys. Chem. A* **2002**, *106*, 3681–3689.
(64) Arenz, S.; Babai, A.; Binnemans, K.; Driesen, K.; Giernoth, R.; Mudring, A.-V.; Nockemann, P. *Chem. Phys. Lett.* **2005**, *402*, 75–79.
(65) Shyamala Devi, V.; Maji, S.; Viswanathan, K. S. *J. Lumin.* **2011**, *131*, 739–748.
(66) AlDamen, M. A.; Clemente-Juan, J. M.; Coronado, E.; Martí-Gastaldo, C.; Gaita-Ariño, A. *J. Am. Chem. Soc.* **2008**, *130*, 8874–8875.
(67) Takamatsu, S.; Ishikawa, T.; Koshihara, S.-y.; Ishikawa, N. *Inorg. Chem.* **2007**, *46*, 7250–7252.
(68) Branzoli, F.; Carretta, P.; Filibian, M.; Zoppellaro, G.; Graf, M. J.; Galan-Mascaros, J. R.; Fuhr, O.; Brink, S.; Ruben, M. *J. Am. Chem. Soc.* **2009**, *131*, 4387–4396.
(69) Chen, X. Y.; Jensen, M. P.; Liu, G. K. *J. Phys. Chem. B* **2005**, *109*, 13991–13999.
(70) Lakshmanan, A. R. *Prog. Mater Sci.* **1999**, *44*, 1–187.
(71) Rukmini, E.; Jayasankar, C. K.; Reid, M. F. *J. Phys.: Condens. Matter* **1994**, *6*, 5919.